Molecular Pharmacology Fast Forward. Published on July 7, 2014 as doi:10.1124/mol.114.093757

Insights into the gating mechanism of the ryanodine-modified human cardiac Ca^{2+} -release channel (RyR2)

Saptarshi Mukherjee, N. Lowri Thomas and Alan J. Williams

Institute of Molecular and Experimental Medicine, Wales Heart Research Institute, Cardiff University School of Medicine, Heath Park, Cardiff, CF14 4XN

Molecular Pharmacology Fast Forward. Published on July 7, 2014 as DOI: 10.1124/mol.114.093757
This article has not been copyedited and formatted. The final version may differ from this version.

Running title: Modified RyR2 gating mechanisms

Corresponding author: Alan J. Williams, Institute of Molecular and Experimental Medicine, Wales Heart Research Institute, Cardiff University School of Medicine, Heath Park, Cardiff, CF14 4XN

Telephone: +442920744430, Fax: +442920743500

Email: williamsaj9@cardiff.ac.uk.

Number of text pages: 38

Number of tables: 2

Number of figures: 8

Number of references: 42

Number of words in the Abstract: 149

Number of words in the Introduction: 737

Number of words in the Discussion: 1499

Abbreviations:

$[Ca^{2+}]$, Ca^{2+} concentration; Ca^{2+}_{cyt}, cytosolic Ca^{2+}; CHAPS 3-[(3-cholamidopropyl)dimethylammonio]-1-propanesulfonic acid; eGFP, enhanced green fluorescent protein; FKBP12.6, FK506 binding protein 12.6; HEDTA, N-{2-[Bis(carboxymethyl)amino]ethyl}-N-(2-hydroxyethyl)glycine; HEK293, human embryonic kidney cells; HMM, hidden Markov model; $IpTx_a$, Imperatoxin A; LL, Log-likelihood; NTA, 2,2',2''-nitrilotriacetic acid; PIPES, 1,4-piperazinediethanesulfonic acid; RyR, ryanodine receptor; RyR2, cardiac ryanodine receptor.

Molecular Pharmacology Fast Forward. Published on July 7, 2014 as DOI: 10.1124/mol.114.093757
This article has not been copyedited and formatted. The final version may differ from this version.

Abstract

Ryanodine receptors (RyRs) are intracellular membrane channels playing key roles in many Ca^{2+}-signaling pathways and, as such, are emerging novel therapeutic and insecticidal targets. RyRs are so named because they bind the plant alkaloid ryanodine with high affinity, and while it is established that ryanodine produces profound changes in all aspects of function, our understanding of the mechanisms underlying altered gating is minimal. We address this issue using detailed single channel gating analysis, mathematical modeling and energetic evaluation of state transitions establishing that, with ryanodine bound, the RyR pore adopts an extremely stable open conformation. We demonstrate that stability of this state is influenced by interaction of divalent cations with both activating and inhibitory cytosolic sites and, in the absence of activating Ca^{2+}, trans-membrane voltage. Comparison of the conformational stability of ryanodine- and Imperatoxin A-modified channels identifies significant differences in the mechanisms of action of these qualitatively similar ligands.

Molecular Pharmacology Fast Forward. Published on July 7, 2014 as DOI: 10.1124/mol.114.093757
This article has not been copyedited and formatted. The final version may differ from this version.

Introduction

Ryanodine receptors (RyR) are ion channels that provide a regulated pathway for the release of signaling Ca^{2+} from intracellular reticular stores. RyR-mediated Ca^{2+} release plays a key role in many signaling processes, the most widely investigated of which is muscle excitation-contraction coupling (Bers, 2002; Lanner et al., 2010). Mutation of the genes encoding both skeletal (RyR1) and cardiac (RyR2) human isoforms results in disease states; the former a metabolic disorder (malignant hyperthermia) or congenital myopathy (central core disease), the latter an arrhythmogenic syndrome (catecholaminergic polymorphic ventricular tachycardia (CPVT)) that can result in sudden cardiac death (Lanner et al., 2010; Venetucci et al., 2012; Amador et al., 2013). These, together with RyR2s altered function in heart failure, have made the channel an emerging target for the pharmaceutical industry, with both novel and existing drugs being proposed as therapeutic agents (Györke and Carnes, 2008; McCauley and Wehrens, 2011). In addition, RyR has become an important target in the agrochemical industry, with a new class of diamide insecticides that selectively target the insect isoform of the receptor (Jeanguenat, 2012). A detailed understanding of the mechanisms of action of these RyR-focused agents and their sites of action on the channel remain to be described, and since sufficient high-resolution structural data is not yet available for this massive tetrameric protein (2.2 MDa) (Lanner et al., 2010; Van Petegem, 2012), information of this kind can only be obtained from detailed analysis of the function of individual RyR channels.

Molecular Pharmacology Fast Forward. Published on July 7, 2014 as DOI: 10.1124/mol.114.093757
This article has not been copyedited and formatted. The final version may differ from this version.

The archetypal RyR ligand is ryanodine and RyR channels are so named because each channel contains a high-affinity binding site for this plant alkaloid (Rogers and Koniuszy, 1948; Fleischer *et al.*, 1985). Thus, investigating the effects of ryanodine on channel gating represents a good starting point in our endeavor to correlate ligand binding with altered channel function. Previous research has identified the structural determinants of the ryanodine molecule that underlie high-affinity binding (Welch et al., 1997), however the location and components of this site in the channel are unknown. Interaction of ryanodine with individual RyR channels results in very profound alterations in channel function; unitary conductance of the channel is reduced while open probability (Po) is increased dramatically (Tinker and Williams, 1993; Lindsay et al., 1994). The mechanisms underlying ryanodine-dependent altered rates of ion translocation in RyR have been described and the structural components of the ryanodine molecule that determine the ryanodine-modified fractional conductance have been investigated (Williams et al., 2001; Welch, 2002). However, the mechanisms involved in the elevation of Po that results from ryanodine's interaction are poorly understood and are the subject of this investigation. The Po of any species of channel is a manifestation of the conformation of its conduction pathway, or more precisely, specific gate regions of the pathway that either prevent, or allow, ions to flow down their electrochemical gradient. The physical identities of gating regions have been established for many K^+ channels from data obtained from combinations of high-resolution crystallographic structural investigations and detailed functional studies (Doyle et al., 1998; Hille, 2001; Roux, 2005). These channels contain two gating regions, one formed by the inner-helix crossover at the cytosolic entrance to the pore and a second within the selectivity filter. The enormous size of the RyR channel, its location in an intracellular membrane and the lack of a

Molecular Pharmacology Fast Forward. Published on July 7, 2014 as DOI: 10.1124/mol.114.093757
This article has not been copyedited and formatted. The final version may differ from this version.

prokaryotic analogue mean that no equivalent structural data is available for RyR, though molecular modeling indicates strong structural similarities between the overall architecture of the pore regions of RyR and K^+ channels (Welch *et al.*, 2004; Ramachandran *et al.*, 2013). In addition, a recent in depth study of channel gating suggested that Ca^{2+} sensitive and insensitive closing transitions could be explained by the presence of two different gates, similar to those found in K^+ channels, in the conduction pathway of RyR2 (Mukherjee et al., 2012).

Here we have carried out detailed analysis of single channel gating and mathematical modeling to reveal novel information about the gating of ryanodine-modified RyR2, which is influenced by different ligands and holding potentials. We also provide the first energetic evaluation of RyR gating in the absence of ligand binding or unbinding and highlight important differences in the mechanisms responsible for elevation of RyR Po by ryanodine and the qualitatively similar effects of the scorpion toxin Imperatoxin A. Together these data emphasize the consequences of ligand interaction on the conformational stability of RyR gating and we discuss how this could influence the structure of the conduction pathway.

Molecular Pharmacology Fast Forward. Published on July 7, 2014 as DOI: 10.1124/mol.114.093757
This article has not been copyedited and formatted. The final version may differ from this version.

Materials and Methods

Cell culture and expression of hRyR2

HEK293 cells were cultured in Dulbecco's modified Eagle's medium supplemented with 10% v/v fetal bovine serum, 2 mM glutamine and 100 μg/ml penicillin/streptomycin. Cells were incubated at 37°C, 5% CO_2 and ~ 80% humidity at a density of $5x10^6$ per 75 cm^2 tissue culture flask 24 hours prior to transfection with pcDNA-3/eGFP-WT hRyR2, using an optimized calcium phosphate method as previously described (Thomas et al., 2004).

Isolation and purification of recombinant hRyR2

Cells were harvested 48 hours post-transfection and lysed on ice in a hypo-osmotic buffer containing (20 mM Tris-HCl, 5 mM EDTA; pH 7.4) containing protease inhibitor cocktail (Roche), by passing it 20 times through a 23G needle. The lysate was subsequently homogenized on ice using a Teflon-glass homogenizer and centrifuged at 1,500 g (Allegra 6R, Beckman) at 4°C for 15 minutes to remove cellular debris. The supernatant was subjected to a high-speed spin (100,000 g) in an Optima L-90K (Beckman) centrifuge at 4°C for 90 minutes. The microsomal pellet thus obtained was solubilized for an hour on ice in a solution containing 1 M NaCl, 0.15 mM $CaCl_2$, 0.1 mM EGTA, 25 mM Na PIPES, 0.6% (w/v) CHAPS and 0.2% (w/v) Phosphatidylcholine (pH 7.4) with protease inhibitor cocktail, 1:1000 (Sigma-Aldrich). The insoluble material was removed by centrifugation at 15,000g for an hour at 4°C. The channel protein was isolated on a 5-30% (w/v) continuous sucrose gradient by centrifugation at 100,000g for 17 hours at 4°C. Fractions containing channel proteins were identified by incorporation into lipid bilayers, before being snap frozen in small aliquots in liquid nitrogen and stored at -80°C until use.

Molecular Pharmacology Fast Forward. Published on July 7, 2014 as DOI: 10.1124/mol.114.093757
This article has not been copyedited and formatted. The final version may differ from this version.

Purification of recombinantly expressed hRyR2 from HEK293 cells ensures the absence of interacting regulatory proteins such as FKBP12.6 and the myocyte specific proteins calsequestrin, junctin and triadin (Stewart et al., 2008).

Single channel recording and data analysis

Single channel experiments were conducted as previously described (Mukherjee et al., 2012). Single hRyR2 channels were incorporated into bilayers formed using suspensions of phosphatidylethanolamine (Avanti Polar Lipids) in n-decane (35 mg/ml). Bilayers were formed in solutions containing 210 mM KCl, 20 mM HEPES (pH 7.4) in both chambers (*cis* and *trans*). An osmotic gradient, which helps the channel protein to incorporate into the bilayer, was created by the addition of two aliquots (100 µl each) of 3 M KCl to the *cis* chamber to which the purified hRyR2 were then added. On stirring, hRyR2 incorporates into the bilayer in a fixed orientation such that the *cis* chamber corresponds to the cytosolic face of the channel and the *trans* chamber to the luminal face. After channel incorporation, symmetrical ionic conditions were re-instated by perfusion of the cis chamber with 210mM KCl. In some experiments, a cytosolic to luminal (*cis* to *trans* side) ionic gradient was used where the *trans* chamber had 210 mM KCl and the cis chamber was perfused with 840 mM KCl. Single channel activity data accumulated from 17 experiments when compared against our recently published hRyR2 Ca^{2+} activation curve (Mukherjee et al., 2012) indicate that the symmetrical 210mM KCl solution used has a "contaminant" [Ca^{2+}] of ~ 1 µM. This was also verified using a calcium probe (Orion, Thermo Scientific). In our experiments the channels were modified using ryanodine (Abcam Biochemicals, UK) and synthetic Imperatoxin A (Alomone Labs, Israel) while their gating behavior was examined under contaminant (~1 µM) or virtually zero Ca^{2+} conditions (extrapolated to ~20 pM free Ca^{2+} as per

Molecular Pharmacology Fast Forward. Published on July 7, 2014 as DOI: 10.1124/mol.114.093757
This article has not been copyedited and formatted. The final version may differ from this version.

http://maxchelator.stanford.edu) using 3.5 mM EGTA on both *cis/trans* sides (the pH remained unaltered at 7.4). In other experiments, the effects of adding 2 mM and 4 mM Ba^{2+} to the cytosolic (*cis*) side on channel gating were examined using $BaCl_2$ stock solutions. The *trans* chamber was held at virtual ground while the *cis* chamber was voltage clamped at ±40 mV in all experiments except when studying voltage dependence where a range of holding potentials were applied. The ambient temperature was 21 ± 2°C in all our experiments. The incorporation of only a single channel in the bilayer was verified in each experiment by modification with ryanodine.

Single channel currents were low-pass filtered at 5 kHz with an 8-pole Bessel filter and then digitized at 20 kHz with a PCI-6036E AD board (National Instruments, TX, USA). Acquire 5.0.1 (Bruxton, WA, USA) was used for viewing and acquisition of the single channel current fluctuations. Data analysis was carried out using the QuB suite of programs version 1.5.0.39 (http://www.qub.buffalo.edu).

Briefly, single channel current traces of 2-3 minutes were idealized employing the Segmental K-means (SKM) algorithm based on Hidden Markov Models (HMM). A dead time of 75-120 μs was imposed during idealization and an initial two state C↔O scheme was used where C denotes a closed state and O an open state. Idealization of the single channel current recordings resulted in the calculation of the mean amplitude, the open probability (Po), median open (T_o) and closed (T_c) durations along with frequency of closings. The Boltzmann equation was used to fit the activity–voltage relationships: $Po(V) = 1/(1 + \exp(z_g F (V - V_{1/2})/RT)$, where Po (V) is the voltage-dependent probability of the voltage sensing element assuming the activated state. V is the bilayer holding potential (in volts), $V_{1/2}$ is the voltage of half-

Molecular Pharmacology Fast Forward. Published on July 7, 2014 as DOI: 10.1124/mol.114.093757
This article has not been copyedited and formatted. The final version may differ from this version.

maximal voltage sensor activation, z_g is the number of elementary charges involved in gating that respond to the voltage drop across the membrane, R is the gas constant (in Joules per Kelvin per mole), and F is the Faraday constant (in Coulombs per mole).

The open and closed dwell time histograms generated by the initial idealization were fitted with a mixture of exponential probability density functions using the Maximum Interval Likelihood (MIL) function of QuB. The MIL program simultaneously optimizes the rate constants for the transitions between the states during fitting of dwell-time histograms by computing the maximum LL of the idealized data, given a model. The program also corrects for missed events that are shorter than the imposed dead time. The kinetic schemes with their respective estimated rates of transitions were used for stochastic simulation of single channel data using the SIM interface of the QuB suite. The simulated data were idealized as described above to confirm the validity of the gating schemes. Statistical methods employed are described in the **Supplemental Methods** section.

Molecular Pharmacology Fast Forward. Published on July 7, 2014 as DOI: 10.1124/mol.114.093757
This article has not been copyedited and formatted. The final version may differ from this version.

Results

Ca^{2+} sensitivity of the ryanodine-modified RyR2

Single channel currents were recorded at ±40 mV holding potential after incorporation of RyR2 in planar lipid bilayers. Channels were activated by ~1 µM Ca^{2+} present in 210 mM KCl solution (pH 7.4) on both sides (cytosolic and luminal) and exhibited typical gating behavior (Po = 0.21 ± 0.06; n=17) (Mukherjee et al., 2012) under these conditions (**Fig. 1A and B**). The channels were subsequently modified to a subconductance state (~60% of full open level) using 1 µM ryanodine on the cytosolic (*cis*) side at +40 mV (**Fig. 1C**). Ryanodine modified channels had a very high Po (~1) with few brief transitions to the closed state, while transitions to the fully open state never occurred (**Fig. 1D and E**). On removal of Ca^{2+} from the cytosolic and luminal side using 3.5 mM EGTA, the frequency of brief closing events from the modified open state increased dramatically. However, this increased propensity of channel closure in the absence of Ca^{2+} had an asymmetric response to voltage, with a marked decrease in channel activity observed at +40, but not at -40 mV, as seen in the representative traces (**Fig.1F and G**). The Po for ryanodine-modified channels activated by 1 µM Ca^{2+} at +40 mV was 0.99 ± 0.002 (n=9) and decreased to 0.75 ± 0.05 (n=9) at nominally zero Ca^{2+} (**Fig. 2A**), while no significant changes were observed at -40 mV (Po = 0.99 ± 0.001 at 1 µM and 0.98 ± 0.009 at nominally zero Ca^{2+}; n=9). The decrease in Po seen at +40 mV is due to an increased frequency of brief closing events (~170 fold increase at +40 mV; **Fig. 2D**) without a change in closed times (mean ~0.4 ms; **Fig. 2B**), leading to a decrease in open times by more than 500 fold at +40 mV (mean open times were 1036 ms and 1.96 ms at 1 µM and zero Ca^{2+} respectively; **Fig. 2C**). A portion of trace **F** in **Fig. 1** is shown on

Molecular Pharmacology Fast Forward. Published on July 7, 2014 as DOI: 10.1124/mol.114.093757
This article has not been copyedited and formatted. The final version may differ from this version.

an expanded time-scale **(Fig. 1H**) to reiterate that the character of the closing events does not change: only their frequency. However, the occurrence of fewer idealized closing events in 1 μM Ca^{2+} at -40 mV, as opposed to +40 mV (see **Figs. 1E** and **D**), causes the closed times to be underestimated (0.26 ± 0.02 ms; n=9, as compared to a mean of ~0.4 ms seen in all other conditions, **Fig. 2B**). Further to this we noted that the increase in the frequency of closing events was due to the removal of Ca^{2+} on the cytosolic side of the channel only, as experiments performed with 1 μM Ca^{2+} on the luminal side (with nominally zero Ca^{2+}_{cyt}) gave the same results (data not shown). The asymmetric response of the ryanodine-modified RyR2 to voltage in the absence of Ca^{2+} was unexpected, as the channel is not known to possess typical voltage sensor domains as seen in other voltage-gated channels (Bezanilla, 2008; Catterall, 2010). Therefore, this voltage dependence of channel gating was explored in detail.

Examination of voltage dependence of modified RyR2 at zero Ca^{2+}

Gating activity of ryanodine-modified channels at nominally zero Ca^{2+} was monitored at a range of holding potentials (-80 mV to +80 mV, at 10 mV increments). The results summarized in **Fig. 3** show a steep dependence of gating kinetics on membrane potential when switched between positive and negative potentials but not with change in the voltage magnitude after the switch. The voltage dependence quickly 'saturates' once the polarity is switched between negative (high Po) and positive (decreased Po) potentials. The Po-voltage relationship obtained (**Fig. 3A**) was fitted with the Boltzmann equation (see **Methods**) which gives the 'apparent gating valence', $\mathbf{z_g}$ of ~ -32 (~ 8 negative charges per subunit). The steepness of this relationship suggests that this mechanism is very fast and is global in nature. The closed times remain unchanged at different holding potentials (**Fig. 3B**) and the mechanism of decrease in Po at positive membrane potentials relative to negative is

Molecular Pharmacology Fast Forward. Published on July 7, 2014 as DOI: 10.1124/mol.114.093757
This article has not been copyedited and formatted. The final version may differ from this version.

by an increase in the frequency of closing events (**Fig. 3D**). To investigate whether this decrease in Po was due to the positive membrane potential or the direction of net ionic flux through the channel (from cytosolic to luminal side) we repeated these experiments in the presence of an ionic gradient (840 mM KCl *cis* and 210 mM KCl *trans*), such that net ionic flux at low negative holding potentials was from the cytosolic to the luminal side of the channel. **Supplemental Figures 2** and **3** show that channel Po was high whether the direction of K^+ flux through the RyR2 was from *cis* to *trans* (-10 mV to -20 mV) or from *trans* to *cis* (-40 mV to -60 mV), with increased closings seen at all positive voltages.

Mathematical modeling and mechanistic basis of modified channel gating

The phenomenon of modal shifts in gating kinetics in RyR has been described in previous studies (Zahradníková and Zahradník, 1995; Armisén et al., 1996) where the channel is shown to spontaneously shift between high and low Po modes; a phenomenon thought to be Ca^{2+} dependent in earlier studies. In the current investigation, modal gating of the ryanodine-modified RyR2 in the virtual absence of Ca^{2+} has been observed and this occurs randomly in time with no obvious triggers (**Supplemental Figure 4**). This stochastic nature of mode shifting implies that it is an intrinsic property of the channel molecule, probably the result of random thermodynamic fluctuations within the channel. For the purposes of describing modified RyR2 gating behavior in terms of mathematical models, these rare periods of very high Po demonstrated in **Supplemental Figure 4** (<5% of total length of recording) were ignored and the typical gating behavior was studied in detail.

Dwell-time histograms generated using the idealized ryanodine-modified single channel data were fitted with exponential probability density functions to generate

Molecular Pharmacology Fast Forward. Published on July 7, 2014 as DOI: 10.1124/mol.114.093757
This article has not been copyedited and formatted. The final version may differ from this version.

kinetic schemes that provide accurate descriptions of gating behavior (see **Methods**). The time constants and areas under fitted exponentials are shown in **Table 1**.

Modified open- and closed-time histograms for single channels activated by 1 μM Ca^{2+} (+40 mV) could be fitted best using one exponential component each (**Fig. 4A**). The channel therefore visits one modified open state (M) and a closed state (C) for the majority of the time i.e. only two most energetically favorable states are resolved (**Scheme I,** annotated as superscript '+' and subscript 'Ca'). The rate constants for the transitions are shown in **Table 2**.

$$M^{+}_{Ca} \underset{k_{CM}}{\overset{k_{MC}}{\rightleftharpoons}} C^{+}_{Ca} \qquad \textbf{Scheme I}$$

The lack of sufficient idealized events at -40 mV (1 μM Ca^{2+}; see **Fig. 1E**) prevented accurate fitting of dwell time histograms, hence a kinetic scheme for channel gating under these conditions is not available.

After removal of Ca^{2+} the frequency of closing events increases, particularly at +40 mV. The fitted dwell time histograms for single channel recordings at +40 mV are shown in **Fig. 4B** where a minimum of two exponential components each is required for the fit. **Scheme IIA** below shows the best fit model for an accurate description of gating behavior where the channel moves between two discrete modified open states M1 and M2 and from these, makes brief but frequent sojourns to corresponding closed states C1 and C2.

Molecular Pharmacology Fast Forward. Published on July 7, 2014 as DOI: 10.1124/mol.114.093757
This article has not been copyedited and formatted. The final version may differ from this version.

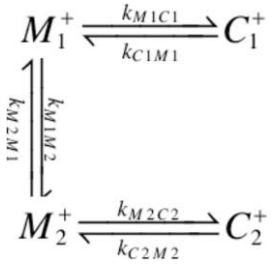

Scheme IIA

The dwell time histograms for single channel data at -40 mV in the absence of Ca^{2+} (**Fig. 4C**) were fitted with one exponential each for open and closed times suggesting a two state mechanism with transitions between a single modified and closed state (**Scheme IIB**). The experimental conditions of zero Ca^{2+} and negative holding potentials are denoted in the scheme as superscript '-' and subscript '0' respectively.

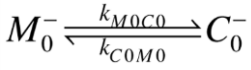

Scheme IIB

Validation of kinetic schemes using model-based simulations

The validity of the gating schemes (**I, IIA and IIB**) obtained by the fitting of dwell time histograms and rate constant optimization were verified by simulation of single channel data. Rate constants from kinetic schemes obtained from individual channels (summarized in **Table 2**) were used for stochastic simulation using the SIM module of QuB interface (see **Methods**). The representative traces shown in **Fig. 5A** are in good agreement with the experimental data traces in **Figure 1**. The change in Po (0.99 ± 0.0006 at +40 mV, 1 μM Ca^{2+}; 0.8 ± 0.03 at +40 mV, nominally zero Ca^{2+}) is due to a decrease in open durations (**Fig. 5D**), while the closed durations remained unaltered (**Fig. 5C**). As in the actual data (**Fig. 2D**), this Po change can only occur due to an increase in the frequency of the closing events. Therefore, the gating models

Molecular Pharmacology Fast Forward. Published on July 7, 2014 as DOI: 10.1124/mol.114.093757
This article has not been copyedited and formatted. The final version may differ from this version.

incorporating the minimum number of states necessary for an accurate description of RyR2 behavior are valid for the experimental conditions used.

Energetic evaluation of state transitions in the modified RyR2

Mathematical modeling is able to resolve only the most stable conformations (wells along the energy landscape) that RyR2 adopts during gating. As insufficient structural data are available to elucidate the mechanisms of state transition in RyR, energetic evaluation of gating could yield valuable information regarding the nature of intermediate transition states. REFER analyses (Grosman, 2002; Zhou et al., 2005) (see **Supplemental Methods** section for a detailed description) were carried out where the equilibrium was perturbed by the complete removal of ligand (Ca^{2+}) or by changing the polarity of the membrane potential. At nominally zero Ca^{2+} the transitions involve a pure gating step as no binding or unbinding of ligand takes place (**Schemes IIA, IIB**). Likewise, with 1 μM Ca^{2+} at +40 mV, the channel activity is saturated (Po~1), therefore, these transitions can also be assumed to be gating steps for all practical purposes (**Scheme I**). The measurement of pure gating steps is important in this analysis, as the inclusion of intermediate binding steps would complicate interpretation of the data (see **Methods**). As we are interested in the properties of transitions to the closed states in both types of perturbations, the modified open states (M, M1 and M2) were chosen as starting states and the closed states (C, C1 and C2) as end states for convenience. As there are two such transitions in Scheme **IIA** with similar characteristics (see **Table 1 and Table 2**), they were considered as two reactions. The log-log plots of the forward rate constants against the equilibrium constants (shown in **Fig. 6)** provide structural clues about the transition state (TS) during the conformational wave from one stable state to another (see **Introduction** and **Supplemental Methods** section). The **Φ** value for the

Molecular Pharmacology Fast Forward. Published on July 7, 2014 as DOI: 10.1124/mol.114.093757
This article has not been copyedited and formatted. The final version may differ from this version.

perturbation due to Ca^{2+} removal ($\mathbf{\Phi_L}$) is close to 1 (**Fig. 6A**), as is that for perturbation of gating equilibrium by a voltage (V_m) switch from -40 to + 40 mV ($\mathbf{\Phi_{\Delta V}}$, **Fig. 6B**). The **Φ** value indicates the structural and temporal nature of the TS relative to the ground states (Auerbach, 2007). A value close to zero would suggest that the structure of TS is similar to the starting ground state (modified state) and that the transition is slow. The results from this study (**Φ** values close to 1) suggest that the conformation of TS is similar to that of the closed end state in both cases and that it occurs early during the course of the reaction (i.e. the transition is quick).

Cytosolic Ba^{2+} as a modulator of ryanodine-modified RyR2 gating

High cytosolic (mM) Ca^{2+} and Ba^{2+} are known to inhibit RyR2 channel gating, probably by acting on low affinity inhibitory sites on the cytoplasmic domain (Laver, 2007; Diaz-Sylvester et al., 2011). Ba^{2+} was used as a tool to further investigate the gating of ryanodine-modified channels in nominally zero Ca^{2+} conditions. Ba^{2+} (2 and 4 mM) was added to the cytosolic side of the channel while holding at -40 mV to prevent any of the divalent from moving to the luminal side. Gating behavior at +40 mV was subsequently studied. The representative traces in **Fig. 7**, show the progressive reduction of modified channel Po brought about by the action of increasing concentrations of Ba^{2+}. Interestingly, with mM Ba^{2+} present at the cytosolic face of the channel, Po is no longer voltage dependent (**Fig. 7, C-F**) with kinetic parameters similar at positive and negative holding potentials (**Fig. 7, G-I**). Po decreases due to both an increase in closed times and a decrease in open times (**Fig. 7H and I**). Fitting of dwell-time histograms using these idealized events reveals the presence two populations of closed events at both positive and negative potentials (**Supplemental Figure 5**); a long closed component (τ = 3.33 ± 0.9 ms; Area = 22 ± 9%; n = 4 at +40 and τ = 3.35 ± 0.7 ms; Area = 27 ± 6%; n = 4 at -40 mV) and a

Molecular Pharmacology Fast Forward. Published on July 7, 2014 as DOI: 10.1124/mol.114.093757
This article has not been copyedited and formatted. The final version may differ from this version.

population of shorter closing events (τ = 0.56 ± 0.09 ms; Area = 78 ± 9% n = 4 at +40 and τ = 0.88 ± 0.13 ms; Amp = 73 ± 6%; n = 4 at -40 mV). These data demonstrate that mM concentrations of cytosolic Ba^{2+} can significantly reduce the Po of ryanodine-modified RyR2 channels. While with ryanodine bound the likelihood of RyR2 channel closing is dramatically reduced, even in the absence of activating levels of cytosolic Ca^{2+}, Ba^{2+} can still interact with the channel and significantly increase the probability of channel closing.

Mechanistic comparison of the action of ryanodine and Imperatoxin A

The scorpion venom toxin Imperatoxin A ($IpTx_a$) stabilizes an open subconductance state of RyR (Tripathy et al., 1998) and it has been proposed that the mechanism of action of $IpTx_a$ is similar to that of ryanodine (Schwartz et al., 2009). The final part of our study compares the action of these ligands under the same experimental conditions. An example of $IpTx_a$ interaction with a Ca^{2+}-activated RyR2 channel is shown in **Supplemental Figure 6**. With $IpTx_a$ bound, the channel resides in a high Po, reduced conductance state. At positive holding potentials the amplitude of the subconductance state is ~30% of the full open state (**Supplemental Figure 6B**), while at negative potentials it is ~40% (**Supplemental Figure 6C**), thereby exhibiting a slight rectification as has been reported previously (Quintero-Hernández et al., 2013). $IpTx_a$ is a reversible modifier of the RyR2 channel, which binds in an activity (Po)-dependent manner. Therefore, the removal of Ca^{2+} after binding of $IpTx_a$ results in permanent channel closure once the toxin unbinds (**Supplemental Figure 6D**), eliminating the probability of further interaction. It is noticeable that following the removal of Ca^{2+} at +40 mV (conditions that produce a significant reduction Po of the ryanodine-modified channel (**Fig. 1F**)), the Po of the $IpTx_a$-modified RyR2 does not change (**Supplemental Figure 6D).** While this observation provides a qualitative

Molecular Pharmacology Fast Forward. Published on July 7, 2014 as DOI: 10.1124/mol.114.093757
This article has not been copyedited and formatted. The final version may differ from this version.

indication that the mechanisms governing altered Po in the ryanodine- and $IpTx_a$-modified channels differ, the very limited amounts of data that can be gathered under these conditions before the channel shuts down precludes a more detailed description of the dependence of $IpTx_a$-modified gating on $[Ca^{2+}]_{cyt}$. To obtain this information we monitored gating parameters in $IpTx_a$-modified states of ryanodine-modified channels. A representative experiment is shown in **Supplemental Figure 7.**

As in earlier experiments, channels were modified with 1 μM ryanodine and Ca^{2+} removed, before being further modified with 20 nM synthetic $IpTx_a$ added to the cytosolic side (**Supplemental Figures 7A, B and C**). Note that the amplitude of the ryanodine-modified subconductance state is distinctly different from that of the $IpTx_a$-modified state of the ryanodine-modified channel. However the $IpTx_a$-modified state observed for the ryanodine-modified RyR2 retains features characteristic of the state prior to ryanodine modification, including a degree of rectification (subconductance of ~30% at +40 mV and ~40% at -40 mV) (**Supplemental Figures 6B, 6C, 7C and 7D)**.

It is evident from the channel traces that once $IpTx_a$ binds, RyR2 ceases to exhibit the gating transitions to the closed state brought about by the complete removal of Ca^{2+} in the ryanodine-modified state at positive holding potentials (**Supplemental Figure 7C)**. The very marked difference in the influence of Ca^{2+} on the gating of the ryanodine- and the $IpTx_a$-modified states of RyR2 seen in these experiments confirms the earlier observation of a lack of Ca^{2+} dependence of the $IpTx_a$-modified state (**Supplemental Figure 6D)**. Disparities between the properties of the ryanodine-modified and $IpTx_a$-modified states are further emphasized by the action of Ba^{2+}. **Supplemental Figures 7E** and **F** demonstrate that gating of the $IpTx_a$-modified state

Molecular Pharmacology Fast Forward. Published on July 7, 2014 as DOI: 10.1124/mol.114.093757
This article has not been copyedited and formatted. The final version may differ from this version.

is insensitive to the inhibitory effect of mM Ba^{2+} that occurs in the ryanodine-modified state of RyR2.

Molecular Pharmacology Fast Forward. Published on July 7, 2014 as DOI: 10.1124/mol.114.093757
This article has not been copyedited and formatted. The final version may differ from this version.

Discussion

Interaction of ryanodine with a single RyR2 channel induces profound changes in function. Unitary conductance is reduced and Po of the reduced-conductance state is increased dramatically. In the presence of activating $[Ca^{2+}]_{cyt}$ Po approaches 1.0 at positive and negative holding potentials. Removal of Ca^{2+}_{cyt} reveals a marked dependence of ryanodine-modified channel Po on voltage, leading to a significant decrease in Po at positive but not negative potentials.

Earlier studies proposed that mechanisms underlying ryanodine-induced elevated Po involved an increase in $[Ca^{2+}]_{cyt}$ sensitivity (Masumiya *et al.*, 2001; Du *et al.*, 2001). The data presented here indicate that this is not the case. In the absence of ryanodine, gating of RyR2 at 1 μM Ca^{2+}_{cyt} is described by a scheme incorporating multiple open and closed states, some of which are Ca^{2+}-dependent and are presumed to be due to the helix-bundle crossover in the channel pore, and one Ca^{2+}-independent transition (flicker closing) thought to be due to fluctuations in the putative selectivity filter region (Mukherjee et al., 2012). Variations in Po induced by changing $[Ca^{2+}]_{cyt}$ result from alterations in closed times, with little change in open times. In contrast, gating of the ryanodine-modified RyR2 can be described by considerably different, simpler schemes in which the relatively small changes in Po arise from variations in open times, while closed times remain constant. These divergent changes in gating would suggest that, rather than sensitizing RyR2 to activating Ca^{2+}, the ryanodine-bound channel adopts an extremely stable modified-open conformation. The stability of this conformation precludes transitions to the full open state and presents a significant energy barrier to closing.

Molecular Pharmacology Fast Forward. Published on July 7, 2014 as DOI: 10.1124/mol.114.093757
This article has not been copyedited and formatted. The final version may differ from this version.

In the presence of activating $[Ca^{2+}]_{cyt}$, Po approaches 1.0 indicating that all potential mechanisms by which the channel can close are disfavored by the presence of ryanodine. Removal of Ca^{2+}_{cyt} partially destabilizes the open conformation resulting in the occurrence of closing events at positive potentials. The brief duration of these closings demonstrates that, even in the absence of activating ligand, the energetically preferred conformation of the ryanodine-bound channel is open. Evidence in support of such a conformational change comes from earlier characterisations of the ion-handling properties of ryanodine-modified RyR2 channels (Tinker and Williams, 1993; Lindsay et al., 1994; Mead and Williams, 2002; Mason et al., 2012). In all cases altered function is consistent with changes in the conformation, stability and rigidity of the channel's conduction pathway.

Removal of Ca^{2+}_{cyt} from the ryanodine-modified RyR2 reveals an underlying dependence of gating on holding potential. A similar effect has been noted previously (Du et al., 2001) and these authors proposed that rather than resulting from a direct influence of voltage on channel gating, luminal to cytosolic cation flux might increase Po. We have tested this proposal by monitoring the dependence of ryanodine-modified RyR2 gating on holding potential in the presence of an ionic gradient. The data are presented in **Supplemental Figures 2** and **3** and demonstrate that irrespective of the direction of ion flow through the channel, in the absence of cytosolic Ca^{2+}, ryanodine-modified RyR2 Po was reduced at positive holding potentials due to an increase in the frequency of closing events. These experiments establish that the observed variations in ryanodine-modified RyR2 gating with changing voltage reflect the ability of the ryanodine-modified conformation of the channel to sense and respond to trans-membrane potential.

Molecular Pharmacology Fast Forward. Published on July 7, 2014 as DOI: 10.1124/mol.114.093757
This article has not been copyedited and formatted. The final version may differ from this version.

Fitting of the Boltzmann equation to the Po-voltage relationship predicts the presence of negatively charged residues that sense the potential drop across the ryanodine-modified channel, thus it is possible that the RyR2 conformation stabilised by ryanodine places acidic residue motifs in locations in which they can sense the trans-membrane potential. By analogy with conventional voltage-sensitive channels, movements of these residues in response to changing potential are transmitted to the gating machinery to alter Po, favoring the open state at negative potentials. The increased tendency for closing at positive potentials is overridden by the interaction of Ca^{2+}_{cyt} with the channel. The Po of the ryanodine-modified conformation is determined by the influence of both trans-membrane potential and $[Ca^{2+}]_{cyt}$. This dependence of channel activity on membrane potential at low Ca^{2+}_{cyt} is not limited to ryanodine-modified RyR: interaction of sulmazole and ATP produce similar effects (Sitsapesan and Williams, 1994; 1995; Laver and Lamb, 1998). The ryanodine-dependent simplification of RyR2 gating, with transitions between modified-open and closed states, has enabled us to use REFER analysis to provide novel insights into the nature of the transition state between these stable, resolvable states. However, due to the enormous size of the channel with potentially complex domain-domain interactions, it is not possible to be certain about the nature of the negatively charged putative voltage sensing motifs.

It has been proposed that the cytosolic domain of the RyR2 channel contains three classes of binding site for Ca^{2+} (Laver, 2007). High affinity (μM) sites are responsible for both increasing (A) and decreasing (I_2) Po, while binding of Ca^{2+}, or other divalent cations, to a low affinity (mM) site (I_1) leads to a reduction in Po. In the absence of

Molecular Pharmacology Fast Forward. Published on July 7, 2014 as DOI: 10.1124/mol.114.093757
This article has not been copyedited and formatted. The final version may differ from this version.

ryanodine, millimolar concentrations of Ba^{2+} added to the cytosolic face of the RyR2 reduce Po (Diaz-Sylvester et al., 2011). This prompted us to use equivalent [Ba^{2+}] to further investigate gating of the ryanodine-modified RyR2 in the absence of Ca^{2+}_{cyt}. We found that cytosolic Ba^{2+}, a) at positive holding potentials, exacerbates the reduction in Po of the ryanodine-modified RyR2 initiated by the removal of Ca^{2+}_{cyt} and b) eliminates the voltage dependence observed in the absence of Ca^{2+}_{cyt}. Lifetime analysis and mathematical modeling indicate that the interaction of Ba^{2+} gives rise to two populations of closed events with equivalent characteristics at both positive and negative potentials.

Reduction in Po of the ryanodine-modified state that results from the interaction of Ba^{2+} is significantly greater than that occurring on removal of activating [Ca^{2+}]. In the absence of Ca^{2+}_{cyt} all three activation/inhibitory binding sites will be available. Ba^{2+}_{cyt} does not activate RyR2 at concentrations between 1 μM and 1 mM (Diaz-Sylvester et al., 2011) and our observation of two Ba^{2+}-dependent closed states indicates that these are likely to result from the binding of Ba^{2+} to the inhibitory sites (I_1 and I_2). The marked increase in closed times associated with the increase in cytosolic Ba^{2+} from 2 to 4 mM suggests that the population of long closings is dependent upon the interaction of Ba^{2+} with the low affinity (I_1) divalent site. Occupancy of the inhibitory sites by Ba^{2+} significantly destabilizes the otherwise stable, rigid, conformation of the ryanodine-modified pore. It should also be noted that Ba^{2+}-dependent closings cannot merely be superimposed onto the closings seen at +40 mV prior to the addition of Ba^{2+}, rather the voltage-dependent closings are replaced by Ba^{2+}-dependent closings and the characteristics of these closings are not influenced by holding potential.

Molecular Pharmacology Fast Forward. Published on July 7, 2014 as DOI: 10.1124/mol.114.093757
This article has not been copyedited and formatted. The final version may differ from this version.

We envisage two possible mechanisms for this behavior. The first is that the presence of mM cytosolic Ba^{2+} effectively removes the voltage-sensing component of the ryanodine-modified conformation of the channel by screening the acidic residues postulated to respond to changing voltage. In the second mechanism the closed states resulting from the interaction of Ba^{2+} with inhibitory sites on RyR2 override the voltage dependence of the ryanodine-modified conformation. This would be analogous to the proposal that the tendency of the ryanodine-modified channel to close at positive potentials is overridden by activating $[Ca^{2+}]_{cyt}$.

The interaction of $IpTx_a$ with RyR2 has functional consequences that appear, superficially, to be analogous to those of ryanodine. However we highlight important differences between the two modified forms of RyR2. The relatively short residence times of $IpTx_a$ on RyR2 following the removal of $Ca^{2+}{}_{cyt}$ make quantification of gating of the $IpTx_a$-modified channel extremely difficult. Nevertheless our data indicate that the Po of the $IpTx_a$-modified RyR2 is not influenced by $[Ca^{2+}]_{cyt}$. We have obtained additional information on the properties of the $IpTx_a$-modified state by monitoring these in ryanodine-bound RyR2 channels. Under these conditions the extremely high Po of the $IpTx_a$-modified state is unaffected by trans-membrane potential, the removal of $Ca^{2+}{}_{cyt}$, or the presence of cytosolic Ba^{2+}. These data indicate that, as is the case with ryanodine, the interaction of $IpTx_a$ with the RyR2 channel stabilizes a modified conformation of the pore-forming region of the channel. However the insensitivity of the $IpTx_a$-bound conformation to factors that alter the stability of the ryanodine-modified channel indicates that the stability of the $IpTx_a$-bound conformation exceeds that of the ryanodine-bound analogue.

Molecular Pharmacology Fast Forward. Published on July 7, 2014 as DOI: 10.1124/mol.114.093757
This article has not been copyedited and formatted. The final version may differ from this version.

The mechanisms underlying profound changes in function associated with the interaction of ryanodine and $IpTx_a$ with the RyR2 channel in relation to divalent cations are summarized in **Fig. 8**. Energetic analysis using REFER reveals new information on the mechanism of state transition during gating of the ryanodine-modified channel. This approach could prove useful in investigating the effects of various RyR agonists and modifiers of function (e.g. phosphorylation, CPVT-linked mutation and RyR-targeted drugs) on the structural stability of the channel as any instability introduced would manifest as a difference in the relationship between ground and transition states in the gating energy landscape, thereby altering the energy barrier. Future studies will determine if these differences can be revealed using the experimental approach established here.

Molecular Pharmacology Fast Forward. Published on July 7, 2014 as DOI: 10.1124/mol.114.093757
This article has not been copyedited and formatted. The final version may differ from this version.

Authorship Contributions

Participated in research design: Mukherjee, Thomas and Williams

Contributed new reagents: Thomas

Conducted experiments: Mukherjee

Performed data analysis: Mukherjee

Wrote or contributed to the writing of the manuscript: Mukherjee, Thomas and Williams

Molecular Pharmacology Fast Forward. Published on July 7, 2014 as DOI: 10.1124/mol.114.093757
This article has not been copyedited and formatted. The final version may differ from this version.

References

Amador FJ, Stathopulos PB, Enomoto M, and Ikura M (2013) Ryanodine receptor calcium release channels: lessons from structure-function studies. *FEBS J* **280**:5456–5470.

Armisén R, Sierralta J, Vélez P, Naranjo D, and Suárez-Isla BA (1996) Modal gating in neuronal and skeletal muscle ryanodine-sensitive Ca^{2+} release channels. *Am J Physiol* **271**:C144–53.

Auerbach A (2007) How to Turn the Reaction Coordinate into Time. *J Gen Physiol* **130**:543–546.

Bers DM (2002) Cardiac excitation-contraction coupling. *Nature* **415**:198–205.

Bezanilla F (2008) How membrane proteins sense voltage. *Nat Rev Mol Cell Biol* **9**:323–332.

Catterall WA (2010) Ion Channel Voltage Sensors: Structure, Function, and Pathophysiology. *Neuron* **67**:915–928.

Diaz-Sylvester PL, Porta M, and Copello JA (2011) Modulation of cardiac ryanodine receptor channels by alkaline earth cations. *PLoS ONE* **6**:e26693.

Doyle DA, Morais Cabral J, Pfuetzner RA, Kuo A, Gulbis JM, Cohen SL, Chait BT, and MacKinnon R (1998) The structure of the potassium channel: molecular basis of K^+ conduction and selectivity. *Science* **280**:69–77.

Du GG, Guo XH, Khanna VK, and MacLennan DH (2001) Ryanodine sensitizes the cardiac Ca^{2+} release channel (ryanodine receptor isoform 2) to Ca^{2+} activation and dissociates as the channel is closed by Ca^{2+} depletion. *Proc Natl Acad Sci USA* **98**:13625–13630.

Fleischer S, Ogunbunmi EM, Dixon MC, and Fleer EA (1985) Localization of Ca^{2+} release channels with ryanodine in junctional terminal cisternae of sarcoplasmic reticulum of fast skeletal muscle. *Proc Natl Acad Sci USA* **82**:7256–7259.

Grosman C (2002) Linear free-energy relationships and the dynamics of gating in the acetylcholine receptor channel. *J Biol Phys* **28**:267–277.

Györke S, and Carnes C (2008) Dysregulated sarcoplasmic reticulum calcium release: potential pharmacological target in cardiac disease. *Pharmacol Ther* **119**:340–354.

Hille B (2001) *Ion Channels of Excitable Membranes*, Sinauer Associates.

Jeanguenat A (2012) The story of a new insecticidal chemistry class: the diamides. *Pest Manag Sci* **69**:7–14.

Lanner JT, Georgiou DK, Joshi AD, and Hamilton SL (2010) Ryanodine Receptors: Structure, Expression, Molecular Details, and Function in Calcium Release. *Cold*

Spring Harbor Perspectives in Biology **2**:a003996–a003996.

Laver DR (2007) Ca^{2+} stores regulate ryanodine receptor Ca^{2+} release channels via luminal and cytosolic Ca^{2+} sites. *Biophysical Journal* **92**:3541–3555.

Laver DR, and Lamb GD (1998) Inactivation of Ca^{2+} Release Channels (Ryanodine Receptors RyR1 and RyR2) with Rapid Steps in [Ca^{2+}] and Voltage. *Biophysical Journal* **74**:2352–2364, Elsevier.

Lindsay AR, Tinker A, and Williams AJ (1994) How does ryanodine modify ion handling in the sheep cardiac sarcoplasmic reticulum Ca^{2+}-release channel? *J Gen Physiol* **104**:425–447.

Mason SA, Viero C, Euden J, Bannister M, West D, Chen SRW, and Williams AJ (2012) The contribution of hydrophobic residues in the pore-forming region of the ryanodine receptor channel to block by large tetraalkylammonium cations and Shaker B inactivation peptides. *J Gen Physiol* **140**:325–339.

Masumiya H, Li P, Zhang L, and Chen SR (2001) Ryanodine sensitizes the Ca^{2+} release channel (ryanodine receptor) to Ca^{2+} activation. *Journal of Biological Chemistry* **276**:39727–39735.

McCauley MD, and Wehrens XHT (2011) Targeting ryanodine receptors for anti-arrhythmic therapy. *Acta Pharmacologica Sinica* **32**:749–757, Nature Publishing Group.

Mead F, and Williams AJ (2002) Ryanodine-induced structural alterations in the RyR channel suggested by neomycin block. *Biophysical Journal* **82**:1964–1974.

Mukherjee S, Thomas NL, and Williams AJ (2012) A mechanistic description of gating of the human cardiac ryanodine receptor in a regulated minimal environment. *J Gen Physiol* **140**:139–158.

Quintero-Hernández V, Jiménez-Vargas JM, Gurrola GB, Valdivia HH, and Possani LD (2013) Scorpion venom components that affect ion-channels function. *Toxicon* **76**:328-342

Ramachandran S, Chakraborty A, Xu L, Mei Y, Samsó M, Dokholyan NV, and Meissner G (2013) Structural determinants of skeletal muscle ryanodine receptor gating. *Journal of Biological Chemistry* **288**:6154–6165.

Rogers EF, and Koniuszy FR (1948) Plant insecticides; ryanodine, a new alkaloid from Ryania speciosa Vahl. *J Am Chem Soc* **70**:3086–3088.

Roux B (2005) Ion Conduction And Selectivity In K^+ Channel. *Annu Rev Biophys Biomol Struct* **34**:153–171.

Schwartz EF, Capes EM, Diego-García E, Zamudio FZ, Fuentes O, Possani LD, and Valdivia HH (2009) Characterization of hadrucalcin, a peptide from Hadrurus gertschi scorpion venom with pharmacological activity on ryanodine receptors. *British Journal of Pharmacology* **157**:392–403.

Sitsapesan R, and Williams AJ (1995) Cyclic ADP-ribose and related compounds activate sheep skeletal sarcoplasmic reticulum Ca^{2+} release channel. *Am J Physiol* **268**:C1235–40.

Sitsapesan R, and Williams AJ (1994) Regulation of the gating of the sheep cardiac sarcoplasmic reticulum Ca^{2+}-release channel by luminal Ca^{2+}. *J Membr Biol* **137**:215–226, Springer.

Stewart R, Song L, Carter SM, Sigalas C, Zaccai NR, Kanamarlapudi V, Bhat MB, Takeshima H, and Sitsapesan R (2008) Single-Channel Characterization of the Rabbit Recombinant RyR2 Reveals a Novel Inactivation Property of Physiological Concentrations of ATP. *J Membr Biol* **222**:65–77.

Thomas NL, George CH, and Lai FA (2004) Functional heterogeneity of ryanodine receptor mutations associated with sudden cardiac death. *Cardiovasc Res* **64**:52–60.

Tinker A, and Williams AJ (1993) Using large organic cations to probe the nature of ryanodine modification in the sheep cardiac sarcoplasmic reticulum calcium release channel. *Biophysical Journal* **65**:1678–1683.

Tripathy A, Resch W, Xu L, Valdivia HH, and Meissner G (1998) Imperatoxin A induces subconductance states in Ca^{2+} release channels (ryanodine receptors) of cardiac and skeletal muscle. *J Gen Physiol* **111**:679–690.

Van Petegem F (2012) Ryanodine receptors: structure and function. *Journal of Biological Chemistry* **287**:31624–31632.

Venetucci L, Denegri M, Napolitano C, and Priori SG (2012) Inherited calcium channelopathies in the pathophysiology of arrhythmias. *Nature Reviews Cardiology* **9**:561–575, Nature Publishing Group.

Welch W (2002) Quantitative relationships between ryanoids, receptor affinity and channel conductance. *Front Biosci* **7**:d1727–42.

Welch W, Rheault S, West DJ, and Williams AJ (2004) A Model of the Putative Pore Region of the Cardiac Ryanodine Receptor Channel. *Biophysical Journal* **87**:2335–2351.

Welch W, Williams AJ, Tinker A, Mitchell KE, Deslongchamps P, Lamothe J, Gerzon K, Bidasee KR, Besch HR, Airey JA, Sutko JL, and Ruest L (1997) Structural components of ryanodine responsible for modulation of sarcoplasmic reticulum calcium channel function. *Biochemistry* **36**:2939–2950.

Williams AJ, West DJ, and Sitsapesan R (2001) Light at the end of the Ca^{2+}-release channel tunnel: structures and mechanisms involved in ion translocation in ryanodine receptor channels. *Q Rev Biophys* **34**:61–104.

Zahradníková A, and Zahradník I (1995) Description of modal gating of the cardiac calcium release channel in planar lipid membranes. *Biophysical Journal* **69**:1780–1788.

Zhou Y, Pearson JE, and Auerbach A (2005) Phi-value analysis of a linear, sequential reaction mechanism: theory and application to ion channel gating. *Biophysical Journal* **89**:3680–3685.

Molecular Pharmacology Fast Forward. Published on July 7, 2014 as DOI: 10.1124/mol.114.093757
This article has not been copyedited and formatted. The final version may differ from this version.

Footnotes

This research was supported by grants from the British Heart Foundation [CH/06/002].

Molecular Pharmacology Fast Forward. Published on July 7, 2014 as DOI: 10.1124/mol.114.093757
This article has not been copyedited and formatted. The final version may differ from this version.

Figure legends

Figure 1. Voltage-dependence of ryanodine-modified RyR2 at zero Ca^{2+}. Representative single channel traces are shown in **(A-H)**. Black bars indicate closed levels; grey bars fully open levels and dotted bars modified levels. An unmodified channel activated by 1 μM (contaminant) cytosolic and luminal Ca^{2+} at + **(A)** and -40 mV **(B)**, subsequently modified with 1 μM ryanodine at +40 mV **(C)**. Under these conditions, the Po of the modified channel is high, with only brief closings at both + **(D)** and – 40 mV **(E)**. Chelation of Ca^{2+} to nominally zero increases the frequency of closing events to a greater degree at +40 **(F)** than -40 mV **(G)**. These closing events are brief in nature, as shown (**H** – x10 expanded section of trace **F**).

Figure 2. Kinetic parameters of ryanodine-modified RyR2 gating (A-D) are represented by black bars (1 μM Ca^{2+}) and grey bars (nominally zero Ca^{2+}). Data are shown as mean ± S.E.M for n=9. * = $p<0.05$; ** = $p<0.005$; n.s= not significant. (**A**) Po is significantly reduced on removal of Ca^{2+} at +40 mV compared to -40 mV. **(B)** Altered Po is not due to a change in Tc (difficulty in resolving events at -40 mV in the presence of 1 μM Ca^{2+} means that Tc was underestimated – see text for details), but instead, **(C)** due to a decrease in To, which despite occurring at both + and -40 mV, only translates into a significant change in **(D)** the frequency of closings at +40 mV.

Figure 3. Detailed examination of ryanodine-modified RyR2 gating in the absence of activating Ca^{2+} at various holding potentials reveals steep voltage dependence. (A) A sharp decrease in channel activity (Po) is seen when holding potential is switched from negative to positive. The data points (closed circles) were

Molecular Pharmacology Fast Forward. Published on July 7, 2014 as DOI: 10.1124/mol.114.093757
This article has not been copyedited and formatted. The final version may differ from this version.

then fitted with a Boltzmann equation (dotted line**).** Due to low signal-to-noise, it is not possible to accurately record single channel currents from ryanodine modified RyR2 below ±20 mV holding potential. The fit of the Boltzmann function was therefore forced to go through the data points near the maximum and minimum levels due to paucity of intermediate data points. This may limit the scope of interpretation from the parameters derived from the fit.

(B) Closed times (Tc) plotted against holding potentials (black squares) do not show significant variation indicating that the character of closing events remain unchanged. **(C)** Modified channel open times (To) decreased sharply at positive holding potentials when switched from negative but don't show much variation at different voltages with the same polarity. **(D)** The frequency of closing events increases at positive voltages and is the basis for the decrease in modified channel Po in response to voltage change. Data presented as mean ± S.E.M with n = 6-9 single channel experiments for each data point. Error bars, where not visible, are included within the symbol.

Figure 4. Fitting of closed and open dwell-time histograms with exponentials allow mechanistic interpretation of single channel data. Representative closed (left) and open (right) time distributions plotted as histograms from a single channel experiment are shown along with their overall fits (solid black curves) and exponential components underneath (grey curves). The membrane potential (±40 mV) and presence/absence of Ca^{2+} is indicated above the distribution. (**A**) The dwell-time distribution of the modified channel in the presence of 1 μM Ca^{2+} at +40 mV was fitted using a single exponential. An insufficient number of events were obtained at -40 mV for an accurate fit. (**B**) At nominally zero Ca^{2+}, two exponential components each were required for fitting closed and open time histograms when the membrane

Molecular Pharmacology Fast Forward. Published on July 7, 2014 as DOI: 10.1124/mol.114.093757
This article has not been copyedited and formatted. The final version may differ from this version.

potential was +40 mV. (**C**) In the absence of Ca^{2+} at -40 mV, only one exponential component each was required for fitting closed and open time histograms. These exponential fits were then associated with corresponding closed and open states in gating models at various conditions of Ca^{2+} and voltage (Schemes I, IIA and IIB). The parameters of fits from many single channel experiments are shown in **Table 1**.

Figure 5. Kinetic parameters from simulated single channel data validate gating models. (A) Representative traces of simulated single channel data generated from the gating schemes. Black solid bars on the left represent the closed level while the grey dotted bars denote the ryanodine-modified open level of RyR2. These simulated traces look similar to their actual experimental counterparts (**Fig. 1D, F, G**). As fitted dwell-time distributions and corresponding gating schemes were unavailable for experiments conducted at -40 mV with 1 μM Ca^{2+} (see Results), simulated traces could not be generated. Analysis of simulated single channel data shows that the results are in agreement with those obtained from experimental data (see **Figure 2** for experimental data). The kinetic parameters are plotted for holding potentials of ±40 mV (hatched dark grey bars, 1 μM Ca^{2+}; light grey bars, nominally zero Ca^{2+}). All data are shown as mean ± S.E.M for n=5 channels. **(B)** Open probabilities at +40 mV at zero Ca^{2+} are significantly lower than when Ca^{2+} is present, or at -40 mV with zero Ca^{2+}. **(C)** Closed times do not show any variation with changes in Ca^{2+} or holding potential. **(D)** The reduction in Po at +40 mV in the absence of Ca^{2+} is due to a significant decrease in open times (235 ± 56 ms; n=5) compared to when Ca^{2+} is present (1.57 ± 0.2 ms; n=5). Significant differences are indicated (** = $p<0.005$).

Molecular Pharmacology Fast Forward. Published on July 7, 2014 as DOI: 10.1124/mol.114.093757
This article has not been copyedited and formatted. The final version may differ from this version.

Figure 6. REFER analysis and Φ (Phi)-value estimation from state transitions provides structural insights into mechanisms. The forward rate constants of the state transitions are plotted against the equilibrium constants on a log-log scale (see **Supplemental Methods** and **Supplemental Figure 1** for details). The rate constants used and the gating schemes they are derived from are shown in **Table 2** and are asterisked. **(A)** In the presence of activating Ca^{2+} at +40 mV when the channel has a Po ~1, the forward rate constant is represented by $\boldsymbol{k_{MC}}$ **(**from Scheme I, red circle in the plot). When Ca^{2+} is removed the perturbation results in decreased Po with two similar forward rate constants $\boldsymbol{k_{M1C1}}$ & $\boldsymbol{k_{M2C2}}$ from Scheme IIA (Black and green circles respectively). The slope of this plot (dotted line) gives the Phi value for ligand-induced perturbation of gating $\boldsymbol{(\Phi_L)}$ = 0.98 ± 0.01 (n=6). **(B)** At -40 mV, in the absence of Ca^{2+}, the Po is high and the forward rate constant is $\boldsymbol{k_{M0C0}}$ from Scheme IIB (Blue square). When the holding potential is switched to +40 mV, the Po decreases and the forward rate constants used are the same as in (A) with $\boldsymbol{k_{M1C1}}$ & $\boldsymbol{k_{M2C2}}$ from Scheme IIA represented by black and green circles respectively. The resulting Phi-value on perturbation of gating due to voltage change $\boldsymbol{(\Phi_{\Delta V})}$ = 0.93 ± 0.02 (n=6). Error bars, where not visible, are included within the dimensions of the closed circles in the plot. All data are shown as mean ± S.E.M.

Figure 7. Cytosolic Ba^{2+} inhibition of ryanodine-modified channel Po also abolishes voltage dependence. Representative single channel traces are shown in **(A-F).** Black bars - closed; grey dotted bars - modified. Modified gating at nominally zero Ca^{2+} at + (**A**) and -40 mV (**B**) (see also Fig. **1F** and **1G**). With 2 mM cytosolic Ba^{2+}, Po is decreased at +40 mV (**C**) and -40 mV (**D**). Increasing Ba^{2+} to 4 mM

Molecular Pharmacology Fast Forward. Published on July 7, 2014 as DOI: 10.1124/mol.114.093757
This article has not been copyedited and formatted. The final version may differ from this version.

further decreases Po at both + (**E**) and -40 mV (**F**). Current amplitude is slightly decreased at +40 mV due to the higher permeability but lower conductance of Ba^{2+} compared with K^+. Parameters from single channel analyses are shown in (**G-I**); blue and red bars represent data at – and +40 mV, respectively. Data are shown as mean ± S.E.M of n = 4-6 channels. Symbols denote significant differences (* = $p<0.05$, ** = $p<0.005$ and *** = $p<0.0001$). (**G**) Voltage dependence of Po is abolished with increasing concentrations of Ba^{2+}, which decrease Po at both + and -40 mV. **(H)** Ba^{2+}-induced decrease in Po results from an increase in closed times at both +40 and -40 mV. This is in contrast to experiments in the absence of Ba^{2+} where closed times remain the same (**Fig. 1**). **(I)** Open times also decrease significantly with Ba^{2+}-induced inhibition of Po to a similar extent at both +40 and -40 mV.

Figure 8. Schematic recapitulation of RyR2 gating behavior under different experimental conditions. The circular cartoon blocks represent the molecular state of the channel: they indicate the channel activity (Po), the ligands interacting with the RyR2 (viz. Ca^{2+}, Ba^{2+}, ryanodine and $IpTx_a$) and the holding potential (±40 mV). Putative binding sites of various interacting ligands are shown as cartoon clouds along the circumference of the blocks; they are either empty (white) or occupied (colored) by the respective ligand. **(A)** For an easier interpretation, the schematic begins at the block with the simplest experimental condition and is marked with a red open diamond sign (❖). Ryanodine-modified RyR2 in the absence of Ca^{2+} (Ca^{2+} binding sites A, I_1 and I_2 are unoccupied) has a lower Po due to an increased frequency of brief closing events at +40 mV when compared to -40 mV. In the presence of 1 μM Ca^{2+} (top row blocks), the putative high affinity activation (A) and inhibition sites (I_2)

Molecular Pharmacology Fast Forward. Published on July 7, 2014 as DOI: 10.1124/mol.114.093757
This article has not been copyedited and formatted. The final version may differ from this version.

on the modified RyR2 are occupied which increases the channel Po to ~1 both at +40 mV and -40 mV with the disappearance of closing events. However, if the ryanodine-modified channel is instead exposed to high cytosolic Ba^{2+} (4 mM) in the absence of Ca^{2+} (arrows pointing downwards in the scheme), the channel is strongly inhibited due to Ba^{2+} occupying both high affinity (I_2) and low affinity (I_1) inhibition sites on the RyR2 (bottom row blocks). Under the influence of Ba^{2+}, voltage dependence of the modified channel gating is abolished (see **Discussion** for possible mechanisms). **(B)** The starting block is marked with a red open diamond sign (❖) as above to represent the simplest experimental scenario describing the interaction of $IpTx_a$ with the channel. In the absence of Ca^{2+}, the $IpTx_a$-modified RyR2 has a very high Po (1.0) with few discernible closing events but once the toxin unbinds, the channel closes, preventing further binding (**Supplemental Figure 6D**). The kinetics of the $IpTx_a$-modified state in the presence of Ca^{2+} does not change and the Po remains ~1.0 (top row left block). Downward arrows from the starting point towards conditions where the RyR2 is modified concomitantly with $IpTx_a$ and ryanodine in the absence of Ca^{2+} at ± 40 mV (as seen in **Supplemental Figures 7C and D**). The Po when $IpTx_a$ is bound to the ryanodine-modified channel still remains at 1.0 with no noticeable change in the kinetics. In contrast, the ryanodine-modified state exhibits voltage dependence of gating as seen in **(a)**. When the above conditions are further modified by the addition of mM Ba^{2+} (bottom row blocks), the $IpTx_a$-modified state of the ryanodine-modified channel remains immune (Po ~ 1.0) to the inhibitory action of the divalent, whereas the Po of the ryanodine-modified state is drastically reduced at both ±40 mV under these conditions.

Molecular Pharmacology Fast Forward. Published on July 7, 2014 as DOI: 10.1124/mol.114.093757
This article has not been copyedited and formatted. The final version may differ from this version.

TABLE 1
The parameters of the exponential components (time constants τ and area A) used in fitting of the open and closed time histograms (see **Fig. 4**) while simultaneously building kinetic schemes (1, 2 and 3) are shown in the table. Each probability density function used in fitting corresponds to a modified open or closed state. Data presented as mean ± S.E.M.

		CLOSED			OPEN	
Conditions		**τ (ms)**	**Area (%)**		**τ (ms)**	**Area (%)**
+40 mV, Scheme I (n=9) 1 μM Ca^{2+}	C_{Ca}	0.33 ± 0.05	100	M_{Ca}	440 ± 91	100
+40 mV, Scheme IIA (n=9) Zero Ca^{2+}	C_1	0.32 ± 0.05	33 ± 7.8	M_1	7.8 ± 2	34 ± 5
	C_2	0.34 ± 0.04	67 ± 7.8	M_2	3.4 ± 0.8	66 ± 5
-40 mV, Scheme IIB (n=6) Zero Ca^{2+}	C_0	0.38 ± 0.04	100	M_0	247 ± 63	100

Molecular Pharmacology Fast Forward. Published on July 7, 2014 as DOI: 10.1124/mol.114.093757
This article has not been copyedited and formatted. The final version may differ from this version.

TABLE 2
Rate constants optimized during fitting of dwell-time histograms and model building.

Gating Schemes and conditions	Rates	Rate constants [a] (mean ± S.E.M)
Scheme 1 Contaminant (~1 μM) Ca^{2+} at +40 mV (n=9)	[b] k_{MC}	5.4 ± 0.9
	k_{CM}	3437 ± 396
Scheme 2 Zero Ca^{2+} at +40 mV (n=9)	k_{M1M2}	42 ± 12.7
	k_{M2M1}	32 ± 6.5
	[b] k_{M1C1}	408 ± 146
	k_{C1M1}	3722 ± 386
	[b] k_{M2C2}	558 ± 88
	k_{C2M2}	3492 ± 413
Scheme 3 Zero Ca^{2+} at -40 mV (n=6)	[b] k_{M0C0}	10.3 ± 3.8
	k_{C0M0}	2764 ± 247

a The units are s^{-1} or $\mu M^{-1}.s^{-1}$ as appropriate.
b Forward rate constants that were used in REFER analysis (**Fig. 6**).

Figure 1.

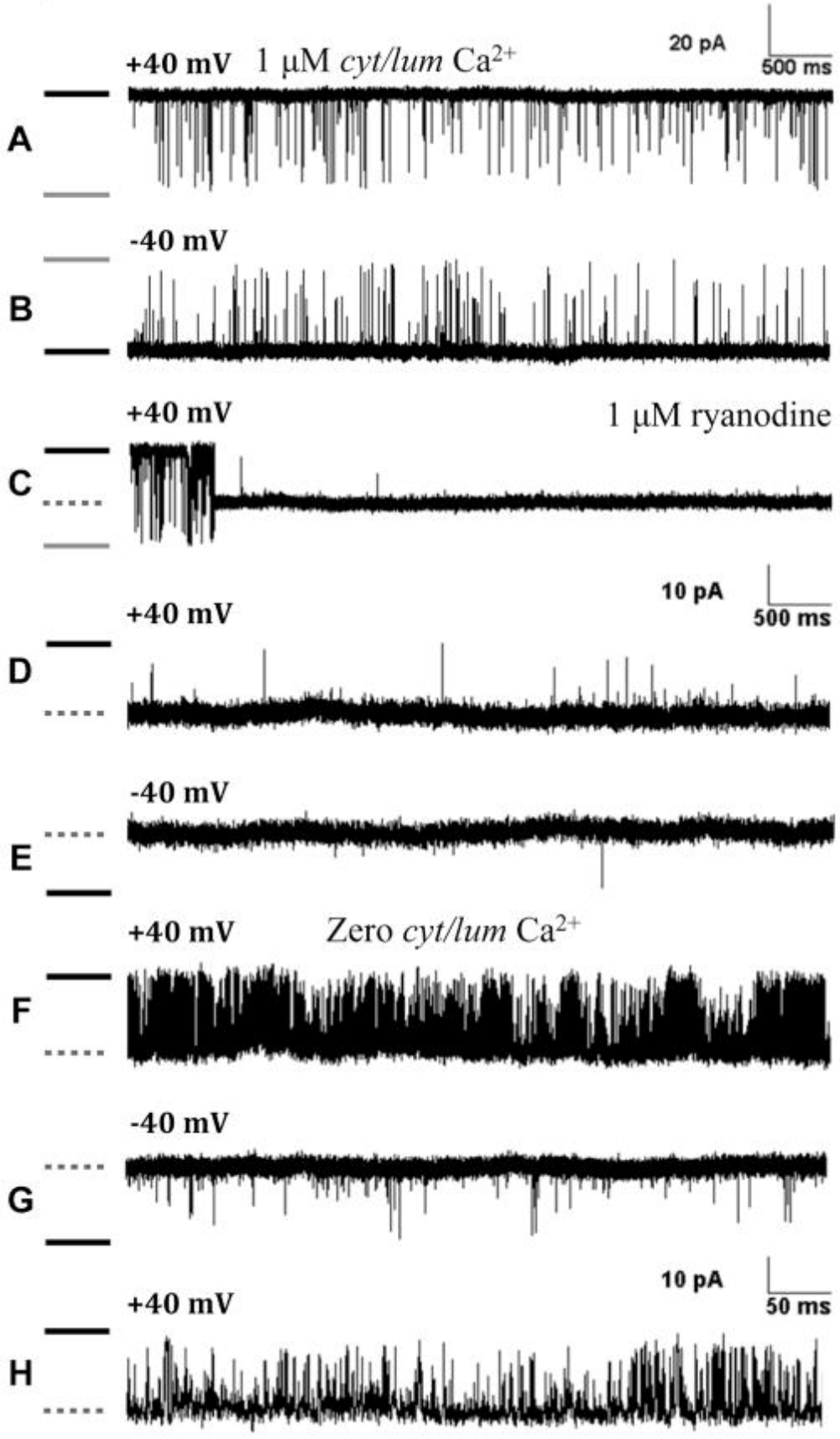
+40 mV
1 μM *cyt/lum* Ca^{2+}
20 pA
500 ms
A
-40 mV
B
+40 mV
1 μM ryanodine
C
10 pA
500 ms
+40 mV
D
-40 mV
E
+40 mV
Zero *cyt/lum* Ca^{2+}
F
-40 mV
G
10 pA
50 ms
+40 mV
H

Figure 2.

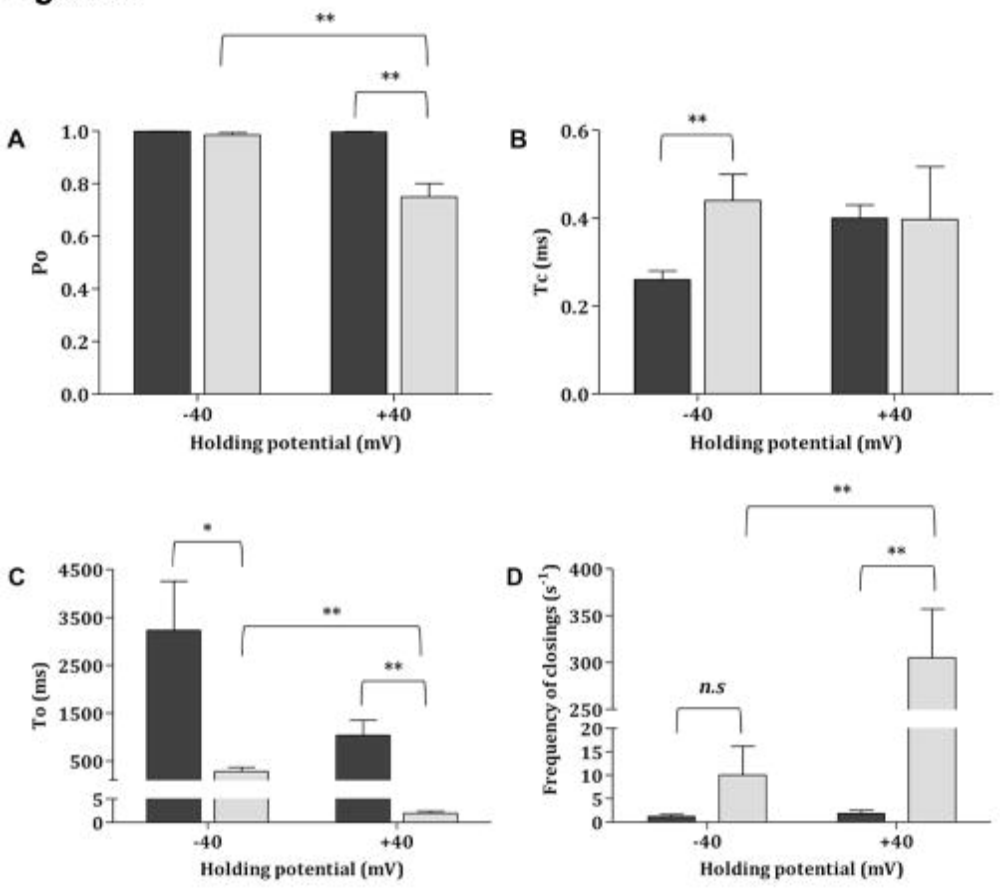
A
Po
1.0
0.8
0.6
0.4
0.2
0.0
**
**
-40
+40
Holding potential (mV)
B
Tc (ms)
0.6
0.4
0.2
0.0
**
-40
+40
Holding potential (mV)
C
To (ms)
4500
3500
2500
1500
500
5
0
*
**
**
-40
+40
Holding potential (mV)
D
Frequency of closings (s-1)
400
350
300
250
20
15
10
5
0
**
**
n.s
-40
+40
Holding potential (mV)

Figure 3.

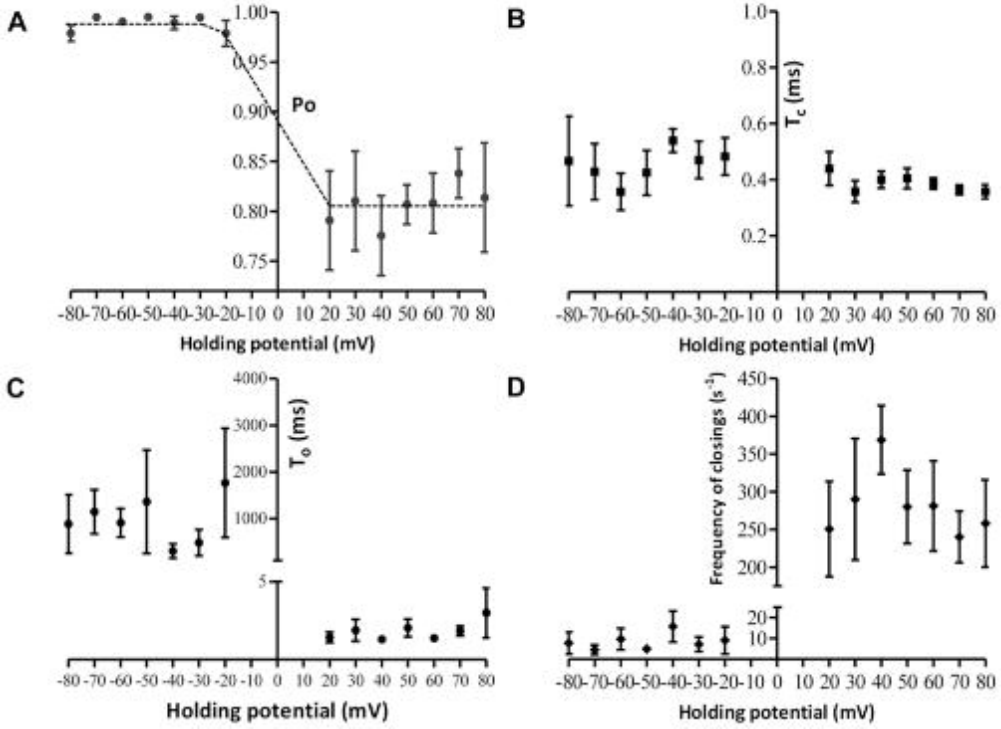
A
Po
1.00
0.95
0.90
0.85
0.80
0.75
-80 -70 -60 -50 -40 -30 -20 -10 0 10 20 30 40 50 60 70 80
Holding potential (mV)
B
T_c (ms)
1.0
0.8
0.6
0.4
0.2
-80 -70 -60 -50 -40 -30 -20 -10 0 10 20 30 40 50 60 70 80
Holding potential (mV)
C
T_o (ms)
4000
3000
2000
1000
5
-80 -70 -60 -50 -40 -30 -20 -10 0 10 20 30 40 50 60 70 80
Holding potential (mV)
D
Frequency of closings (s^{-1})
450
400
350
300
250
200
20
10
-80 -70 -60 -50 -40 -30 -20 -10 0 10 20 30 40 50 60 70 80
Holding potential (mV)

Figure 4.

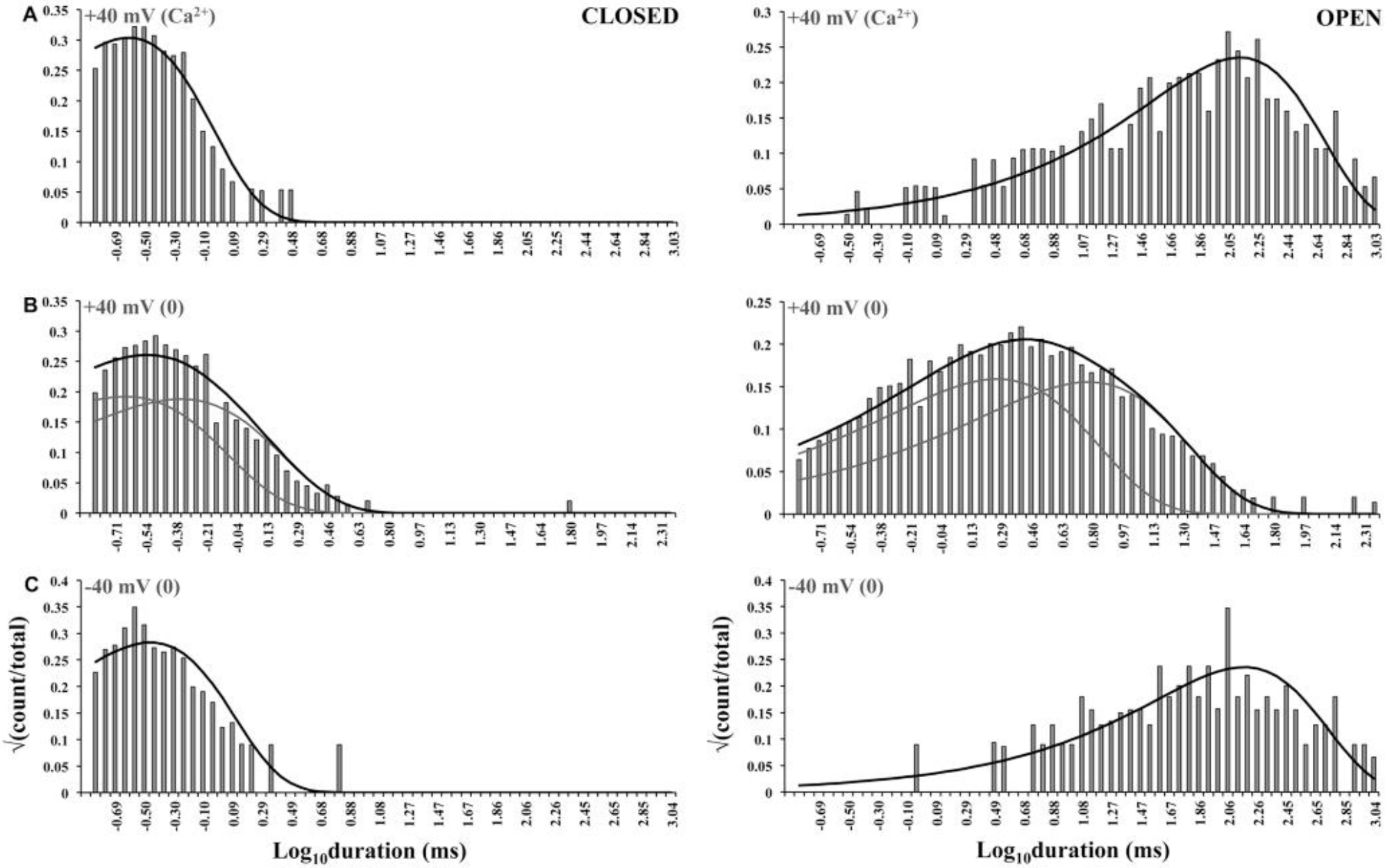
A
+40 mV (Ca2+)
CLOSED
+40 mV (Ca2+)
OPEN
B
+40 mV (0)
+40 mV (0)
C
-40 mV (0)
-40 mV (0)
√(count/total)
√(count/total)
Log10duration (ms)
Log10duration (ms)

Figure 5.

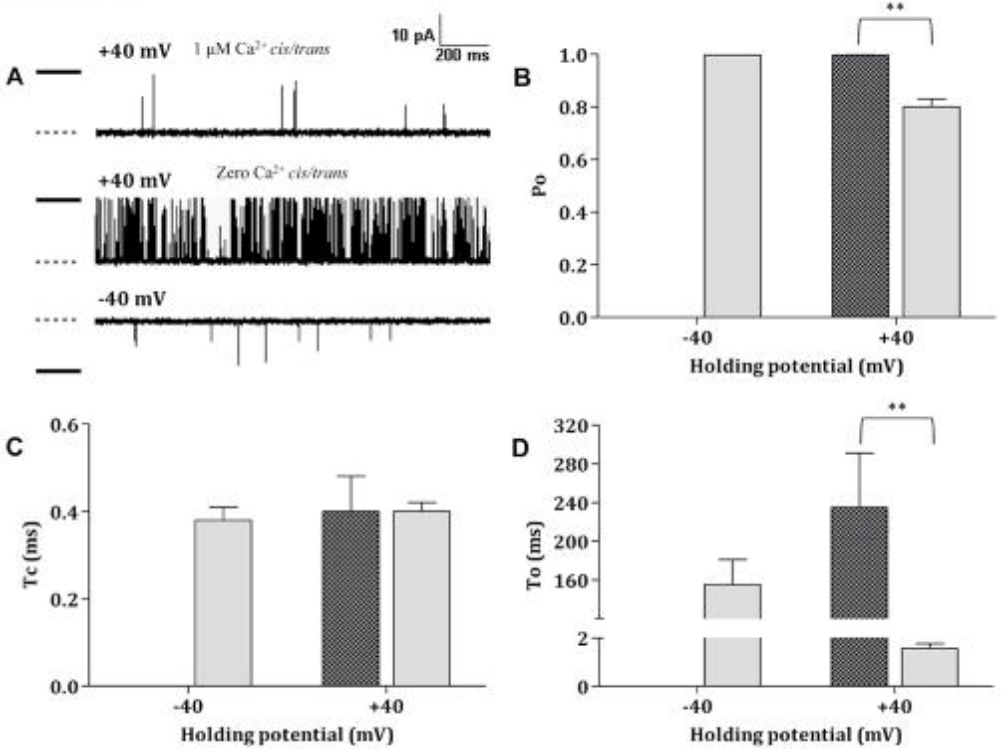
A
+40 mV
1 μM Ca2+ cis/trans
10 pA
200 ms
+40 mV
Zero Ca2+ cis/trans
-40 mV
B
**
Po
1.0
0.8
0.6
0.4
0.2
0.0
-40
+40
Holding potential (mV)
C
Tc (ms)
0.6
0.4
0.2
0.0
-40
+40
Holding potential (mV)
D
**
To (ms)
320
280
240
200
160
2
0
-40
+40
Holding potential (mV)

Figure 6.

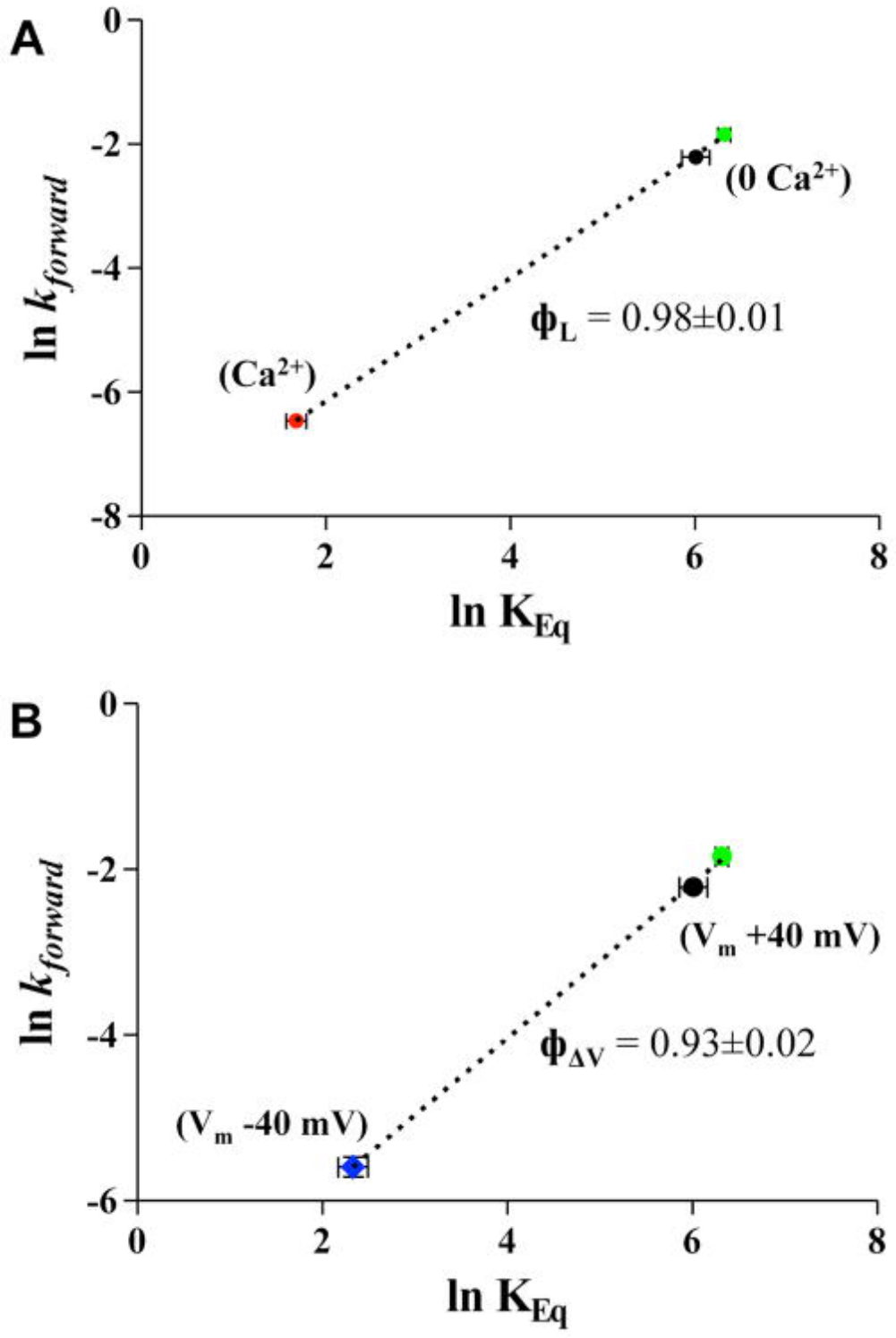
A
0
-2
-4
-6
-8
ln $k_{forward}$
(0 Ca^{2+})
ϕ_L = 0.98±0.01
(Ca^{2+})
0
2
4
6
8
ln K_{Eq}
B
0
-2
-4
-6
ln $k_{forward}$
(V_m +40 mV)
$\phi_{\Delta V}$ = 0.93±0.02
(V_m -40 mV)
0
2
4
6
8
ln K_{Eq}

Figure 7.

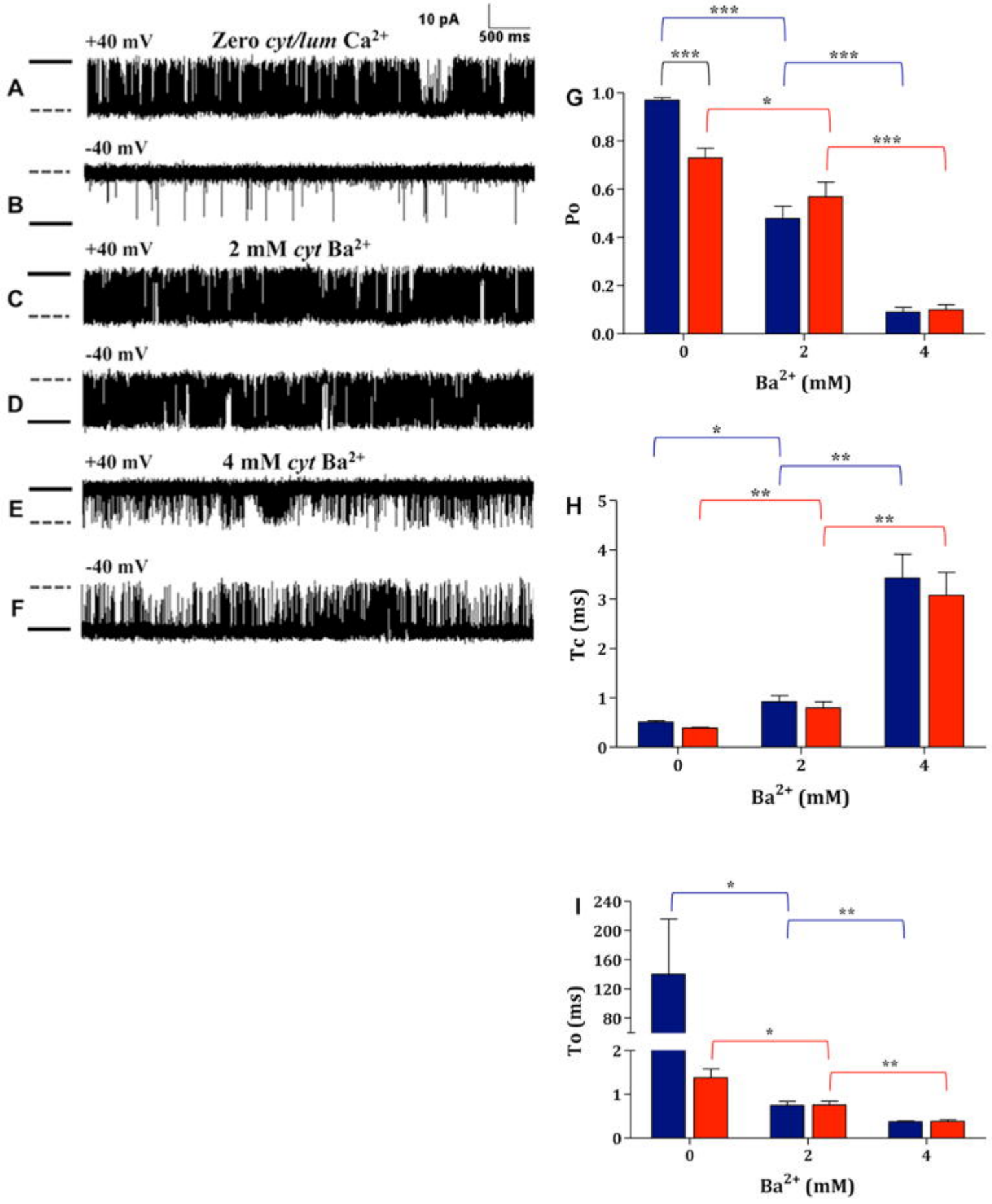
10 pA
500 ms
+40 mV
Zero cyt/lum Ca2+
A
-40 mV
B
+40 mV
2 mM cyt Ba2+
C
-40 mV
D
+40 mV
4 mM cyt Ba2+
E
-40 mV
F
G
Po
Ba2+ (mM)
H
Tc (ms)
Ba2+ (mM)
I
To (ms)
Ba2+ (mM)

Figure 8.

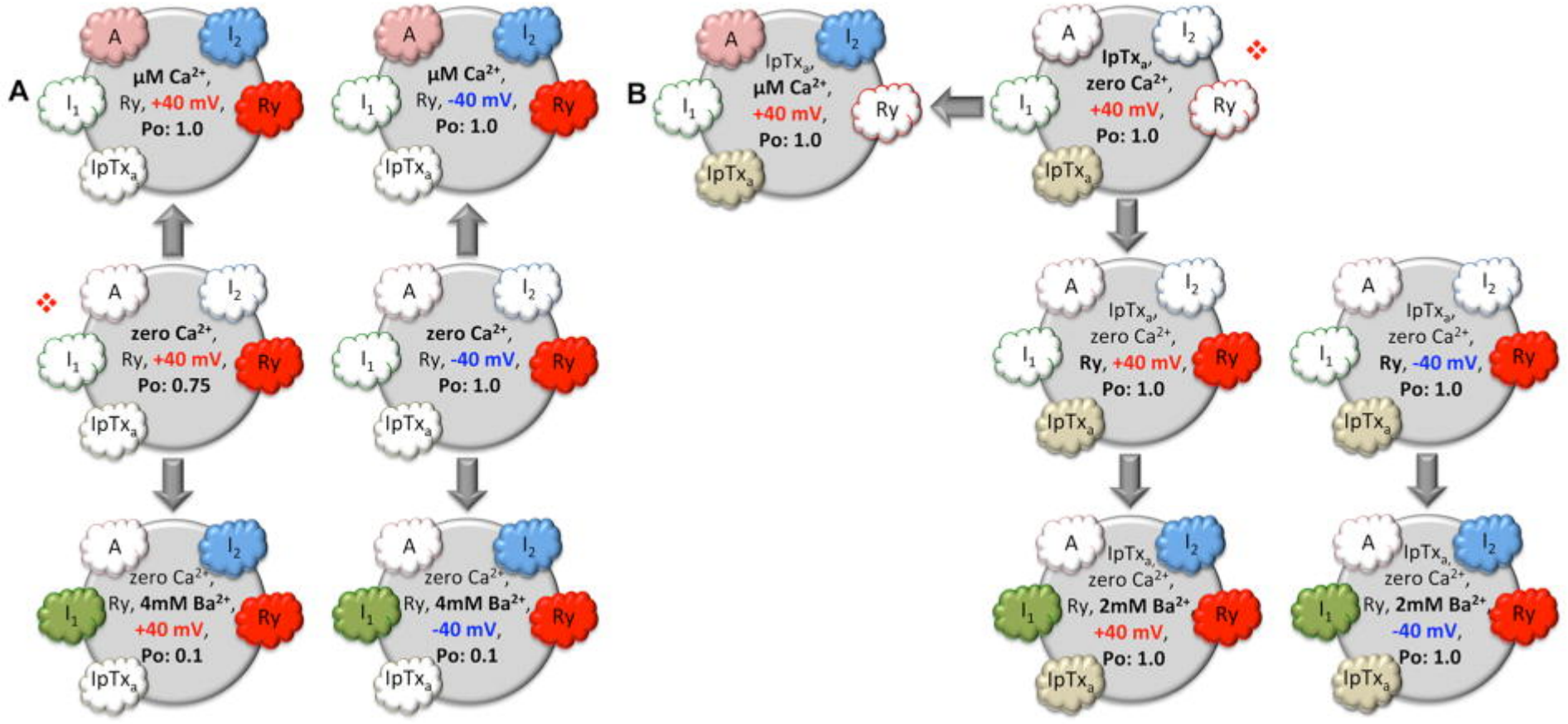
A
μM Ca2+, Ry, +40 mV, Po: 1.0
μM Ca2+, Ry, -40 mV, Po: 1.0
zero Ca2+, Ry, +40 mV, Po: 0.75
zero Ca2+, Ry, -40 mV, Po: 1.0
zero Ca2+, Ry, 4mM Ba2+, +40 mV, Po: 0.1
zero Ca2+, Ry, 4mM Ba2+, -40 mV, Po: 0.1
B
IpTxa, μM Ca2+, +40 mV, Po: 1.0
IpTxa, zero Ca2+, +40 mV, Po: 1.0
IpTxa, zero Ca2+, Ry, +40 mV, Po: 1.0
IpTxa, zero Ca2+, Ry, -40 mV, Po: 1.0
IpTxa, zero Ca2+, Ry, 2mM Ba2+, +40 mV, Po: 1.0
IpTxa, zero Ca2+, Ry, 2mM Ba2+, -40 mV, Po: 1.0